Lattice dynamics of two-dimensional colloidal crystals subject to external light potentials

H. H. von Grünberg
Institut für Chemie, Karl-Franzens-Universität, Graz, Austria

J. Baumgartl
2. Physikalisches Institut, Universität Stuttgart, Stuttgart, Germany

(Received 29 October 2006; published 22 May 2007)

By exposing two-dimensional crystals to tunable substrate potentials one can selectively manipulate the crystal's phonon band structure. We explore this idea and study the overdamped lattice dynamics of colloidal crystals subject to commensurate substrate potentials with sinusoidal modulations in up to two spatial directions. We furthermore show that the mean-square displacement of colloids in the crystal can be understood as the Laplace transform of the phonon spectrum and discuss how our results can best be verified experimentally.

DOI: 10.1103/PhysRevE.75.051406 PACS number(s): 82.70.Dd, 63.20.Dj, 63.22.+m

I. INTRODUCTION

A two-dimensional (2D) colloidal suspension is an ideal model system to study various properties of 2D solids, such as their elastic behavior and the phonon band structure [1], but also more fundamental properties that are related to the melting transition in 2D [2,3]. The reasons why colloidal systems have been chosen for these studies are obvious; their size and nature allow one, first, to easily tune the shape and strength of the colloidal interaction and, second, to directly observe the particles under a microscope—a property which permits application of such a powerful tool as the video-microscopy technique.

However, physical systems in strictly two dimensions are rare in nature. Two-dimensional systems are more likely to occur in the presence of some sort of substrate. A good example for such combined systems are films—i.e., layers of particles (ideally monolayers) adsorbed onto substrates [4]. Again, colloidal suspensions can serve as model systems, because substrates can be realized in various different ways. A prominent example is an optical tweezer which allows the trapping of colloids by laser beams [5]. Extended substrate patterns can also be realized by interfering expanded laser beams [6] or by scanning focused laser beams. Thereby, the strength of the substrate potential can be tuned continuously over a large range, simply by changing the intensity of the laser beam.

The present work extends the theoretical framework of 2D lattice dynamics to systems where a 2D crystal is additionally subjected to a substrate potential. Specifically, we ask whether or not it is possible to "tailor" phonon band structures of 2D crystals by tuning the substrate potential. Having in mind the experimental realization of our ideas, we consider 2D colloidal crystals interacting with substrate potentials that result from patterns of interfering laser beams and calculate band structure, phonon spectrum, and elastic constants of these crystals. The substrate potentials are assumed to have sinusoidal modulations with wave vectors pointing to lattice sites of the reciprocal lattice; i.e., the wavelength and direction of these modulations match the direction of, and distance between, lattice lines of the crystal. As a result of the interaction between the colloids and these commensurate substrate potentials, the usual system of "springs" between the particles resulting from the colloidal interaction is augmented by an additional system of tunable and oriented springs connecting each particle to its lattice site.

We find that bands can be reformed in many different ways: they can be flattened or simply shifted without changing their shape. It is even possible to manipulate all bands in such a way that the original band structure of the free crystal reappears, only that it is shifted by a certain value. However, this shift turns out to be essential as it leads to a mean-square displacement that no longer diverges as it would in a free crystal. In other words, while an unconstrained 2D crystal lacks perfect order (and should therefore better be called a "solid" rather than a "crystal"), we here demonstrate how to obtain a 2D crystal with exactly the same particle-particle interaction as the free crystal, which, however, is showing perfect order and a nondiverging mean-square displacement.

Our work also adds a new aspect to the research that has been done on 2D colloidal fluids interacting with light fields. Such a system was first investigated by Chowdhury *et al.* [6] who showed that a sufficiently large potential induces a phase transition to a structure which exhibits solidlike order. Related experimental studies deal with topics such as laser-induced freezing and melting [7–9], strain-induced domain formation [10], and melting of 2D colloidal systems exposed to 1D periodic light fields [11,12] or to periodic pinning arrays with square symmetry [13]. Other studies investigate the interaction of a system of colloidal "molecules" which are arranged on regular lattices created by light potentials [14].

The paper is organized as follows. After briefly summarizing the essentials of the theory of lattice dynamics in Sec. II, we formulate in Sec. III the Langevin equation for colloidal crystals in the overdamped limit. Section IV is then devoted to calculating the band structure of a hexagonal crystal subject to substrate potentials. Discussing first the case of a free crystal, we explain in Sec. IV B our assumptions concerning the substrate potential and discuss in Sec. IV C the band structure and phonon spectrum for crystals exposed to various combinations of different substrate potentials. There are several ways to access experimentally the phonon band structure of colloidal crystals. We briefly discuss these possibilities in Sec. V. One way is to determine the phonon spectrum from a measurement of the mean-square displace-

ment of the colloids in the crystal which in Sec. V A we show to be connected to the phonon spectrum through a Laplace transformation. Section VI finally discusses the question whether the elasticity of 2D matter can be modified externally in the same way as the band structure.

II. THEORY OF LATTICE DYNAMICS

To introduce our notation we start by briefly recapitulating the essentials of the classical theory of lattice dynamics [24]. We consider a 2D crystalline system of Brownian particles subject to a commensurate external potential. Let $\vec{R}(l)$ be the vector pointing to the lattice site l and $\vec{R}(ll')=\vec{R}(l)-\vec{R}(l')$ the difference vector between two lattice points. The displacement of a particle from $\vec{R}(l)$ is denoted by $\vec{u}(l)$, so that $\vec{r}(l)=\vec{R}(l)+\vec{u}(l)$ is the position of particle l. In the harmonic approximation, the total potential interaction energy V of the system is approximated by the expansion

$$V = V(0) + \frac{1}{2}\sum_{l,l',\alpha,\beta} \Phi_{\alpha\beta}(ll')u_\alpha(l)u_\beta(l'), \tag{1}$$

where

$$\Phi_{\alpha\beta}(ll') = \left.\frac{\partial^2 V}{\partial u_\alpha(l)\partial u_\beta(l')}\right|_{\text{eq}} \tag{2}$$

is the second derivative of V with respect to the displacements $u_\alpha(l)$ and $u_\beta(l')$ $(\alpha,\beta=x,y)$, to be taken in the equilibrium configuration. The sum over l and l' in Eq. (1) is over all N-lattice sites of the system; the static term $V(0)$ in this equation is not relevant in the present context and is set to zero while the linear term in the expansion has already been omitted as it must vanish in an equilibrium configuration. The potential energy V is the sum of two terms: one term V^L arising from the external potential created by the laser light and another term V^0 that results from the interaction between the particles of the free crystal. Correspondingly, $\Phi_{\alpha\beta}(ll')$ splits into $\Phi^0_{\alpha\beta}(ll')$ and $\Phi^L_{\alpha\beta}(ll')$, where further below it is shown that the latter quantity is diagonal in l. Hence,

$$\Phi_{\alpha\beta}(ll') = \Phi^0_{\alpha\beta}(ll') + \Phi^L_{\alpha\beta}\delta_{ll'}. \tag{3}$$

Consideration of a rigid-body translation of the free crystal leads to the relation

$$\sum_{l'} \Phi^0_{\alpha\beta}(ll') = \sum_{l'} \Phi^0_{\alpha\beta}(0l') = 0, \tag{4}$$

which implies that

$$\sum_{l'} \Phi_{\alpha\beta}(0l') = \Phi^L_{\alpha\beta}. \tag{5}$$

With $\Phi_{\alpha\beta}(ll')$ we come to the dynamical matrix of our problem,

$$D_{\alpha\beta}(\vec{q}) = \sum_{l'} \Phi_{\alpha\beta}(ll')e^{i\vec{q}\cdot\vec{R}(l'l)} = \sum_{l'} \Phi_{\alpha\beta}(0l')e^{i\vec{q}\cdot\vec{R}(l')}, \tag{6}$$

which, like $\Phi_{\alpha\beta}(ll')$ in Eq. (3), decomposes into two terms,

$$D_{\alpha\beta}(\vec{q}) = D^0_{\alpha\beta}(\vec{q}) + D^L_{\alpha\beta}(\vec{q}). \tag{7}$$

Let $\lambda(\vec{q}j)$ be the jth eigenvalue of $D_{\alpha\beta}(\vec{q})$ $(j=1,2)$ and $\vec{e}(\vec{q}j)$ the corresponding eigenvector. Hence,

$$\sum_\beta D_{\alpha\beta}(\vec{q})e_\beta(\vec{q}j) = \lambda(\vec{q}j)e_\alpha(\vec{q}j), \tag{8}$$

where $e_\alpha(-\vec{q}j)=e^*_\alpha(\vec{q}j)$ and

$$\sum_\beta e^*_\beta(\vec{q}j)e_\beta(\vec{q}j') = \delta_{jj'}, \quad \sum_j e^*_\alpha(\vec{q}j)e_\beta(\vec{q}j) = \delta_{\alpha\beta}. \tag{9}$$

We are now in the position to transform $u_\alpha(l)$ to symmetry-adapted coordinates,

$$Q(\vec{q}j) = \frac{1}{\sqrt{N}}\sum_{l,\alpha} u_\alpha(l)e^*_\alpha(\vec{q}j)e^{-i\vec{q}\cdot\vec{R}(l)}, \tag{10}$$

$$u_\alpha(l) = \frac{1}{\sqrt{N}}\sum_{\vec{q},j} Q(\vec{q}j)e_\alpha(\vec{q}j)e^{i\vec{q}\cdot\vec{R}(l)}, \tag{11}$$

where again $Q(-\vec{q}j)=Q^*(\vec{q}j)$. The sum over $\vec{q}$ in Eq. (11) is to be understood as the usual sum over the discrete set of N allowed $\vec{q}$ values. We recall that

$$\frac{1}{N}\sum_{\vec{q}} e^{-i\vec{q}\cdot\vec{R}(l'l)} = \delta_{ll'}, \quad \frac{1}{N}\sum_{l} e^{-i(\vec{q}-\vec{q}')\cdot\vec{R}(l)} = \delta_{\vec{q}\vec{q}'}. \tag{12}$$

Introducing the discrete Fourier transform of $u_\alpha(l)$,

$$u_\alpha(\vec{q}) = \frac{1}{\sqrt{N}}\sum_{l} u_\alpha(l)e^{-i\vec{q}\cdot\vec{R}(l)}, \tag{13}$$

we can write Eq. (10) in a more compact form as

$$Q(\vec{q}j) = \vec{e}^*(\vec{q}j)\cdot\vec{u}(\vec{q}). \tag{14}$$

With Eqs. (9), (11), and (12), Eq. (1) can now be written as

$$V = \frac{1}{2}\sum_{\vec{q},j} \lambda(\vec{q},j)|Q(\vec{q}j)|^2. \tag{15}$$

III. LANGEVIN EQUATION FOR COLLOIDAL CRYSTALS

To further prepare our considerations below, we next introduce an equation of motion for a colloidal particle in the crystal. Colloidal crystals differ from atomic crystals not only in particle size and lattice constant but also regarding the dynamics, which is different due to the hydrodynamic interaction that arises when moving colloidal particles exchange momentum through the solvent. The viscous solvent causes friction, which strongly dampens the lattice vibrations [16,18]. Hydrodynamics and the phonon dispersion curves of overdamped colloidal crystals have been studied experimentally using dynamic light scattering [15–19]. Theoretically, the lattice dynamics of colloidal systems has been treated in analogy with solid-state theory, the only modification being the incorporation of friction and hydrodynamics. For lattice dynamic theories with hydrodynamic interaction, see

[16,20–23]. We here follow the Langevin treatment of the lattice dynamics first suggested by Hurd *et al.* [16], but ignore hydrodynamic interactions and include just the simple Stokes friction. For an even more simplified dynamical description of colloids in crystals see [25].

We consider the Langevin equation in the overdamped limit which reads

$$\gamma \frac{\partial u_\alpha(l)}{\partial t} = -\frac{\partial V}{\partial u_\alpha(l)} + f_\alpha(l,t), \tag{16}$$

with $\alpha \in \{x,y\}$ and γ being the friction coefficient. Here, $f_\alpha(l)$ is the usual stochastic force for which we assume that

$$\langle f_\alpha(l,t)\rangle = 0, \quad \langle f_\alpha(l,t) f_{\alpha'}(l',t+\tau)\rangle = \epsilon\delta(\tau)\delta_{ll'}\delta_{\alpha\alpha'}, \tag{17}$$

with a constant ϵ to be specified later. Replacing in Eq. (10) $u_\alpha(l)$ by $f_\alpha(l)$, we obtain the conjugate of $f_\alpha(l)$, denoted in the following by $F(\vec{q}j)$. Using Eqs. (9) and (12), one can show that Eq. (17) translates into

$$\langle F(\vec{q}j,t)\rangle = 0, \quad \langle F^*(\vec{q}j,t) F(\vec{q}'j',t+\tau)\rangle = \epsilon\delta(\tau)\delta_{\vec{q}\vec{q}'}\delta_{jj'}. \tag{18}$$

Using Eq. (1) in Eq. (16) we obtain

$$\gamma \dot{u}_\alpha(l) - f_\alpha(l) + \sum_{l',\beta} \Phi_{\alpha\beta}(ll') u_\beta(l') = 0. \tag{19}$$

Replacing now $u_\alpha(l)$ and $f_\alpha(l)$ by their respective expression (11),

$$\sum_{\vec{q},j} \Bigg[\{\gamma\dot{Q}(\vec{q}j) - F(\vec{q}j)\} e_\alpha(\vec{q}j) e^{i\vec{q}\cdot\vec{R}(l)} + Q(\vec{q}j) \sum_\beta e_\beta(\vec{q}j) \sum_{l'} \Phi_{\alpha\beta}(ll') e^{i\vec{q}\cdot\vec{R}(l')} \Bigg] = 0 \tag{20}$$

and using then Eq. (8) we find

$$\sum_{\vec{q},j} [\{\gamma\dot{Q}(\vec{q}j) - F(\vec{q}j) + Q(\vec{q}j)\lambda(\vec{q}j)\} e_\alpha(\vec{q}j) e^{i\vec{q}\cdot\vec{R}(l)}] = 0, \tag{21}$$

where we had to insert $1 = e^{i\vec{q}\cdot\vec{R}(l)} e^{-i\vec{q}\cdot\vec{R}(l)}$. Because of Eqs. (9) and (12), we can conclude that

$$\gamma\dot{Q}(\vec{q}j) - F(\vec{q}j) + Q(\vec{q}j)\lambda(\vec{q}j) = 0, \tag{22}$$

which is the equation which our considerations in Sec. V A are based on.

IV. BAND STRUCTURE OF A HEXAGONAL CRYSTAL SUBJECT TO A SUBSTRATE POTENTIAL

The set of eigenvalues $\lambda(\vec{q}j)$ of the dynamical matrix corresponding to a particular j forms the jth band, while the set of bands constitutes the phonon band structure. This band structure is calculated in this section for our problem at hand. We start by first considering $D^0_{\alpha\beta}(\vec{q})$ in Eq. (7)—i.e., the dynamical matrix of a free hexagonal crystal.

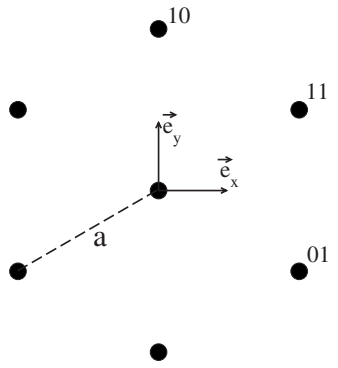

FIG. 1. Unit vectors $\vec{e}_x$ and $\vec{e}_y$, lattice constant a, and the first-neighbor shell lattice points of a hexagonal lattice.

A. Free crystal

For a system with particles interacting with central forces, $\Phi^0_{\alpha\beta}(0l)$ takes the form (Eq. 29.3 in [24]),

$$\Phi^0_{\alpha\beta}(0l) = \left[-p_1(R)\delta_{\alpha\beta} - p_2(R)\frac{R_\alpha R_\beta}{R^2} \right]_{\vec{R}(l0)}, \tag{23}$$

where R is the modulus of the vector with component R_α or R_β. This expression has to be evaluated at the relative lattice vector $\vec{R}(l0) = \vec{R}(l)$. To simplify the notation we have introduced the two functions

$$p_1(r) = \frac{\phi'(r)}{r}, \quad p_2(r) = \phi''(r) - \frac{\phi'(r)}{r}, \tag{24}$$

where $\phi(r)$ is the pair interaction potential between two colloidal particles at a distance r while the prime denotes the derivative of $\phi(r)$ with respect to r.

In the following we need the three unit vectors pointing to the lattice points (10), (11), and (01) of a hexagonal lattice (see Fig. 1),

$$\hat{\vec{e}}_{10} = \vec{e}_y, \quad \hat{\vec{e}}_{11} = \frac{\sqrt{3}}{2}\vec{e}_x + \frac{1}{2}\vec{e}_y, \quad \hat{\vec{e}}_{01} = \hat{\vec{e}}_{11} - \hat{\vec{e}}_{10}. \tag{25}$$

As a short hand notation of these three vectors we introduce $\hat{\vec{e}}_\nu$ with the index ν referring to the indices of the three lattice sites, $\nu = 1,2,3 = (10),(11),(01)$. The remaining three lattice sites $(-1,0)$, $(-1,-1)$, and $(0,-1)$ of the first-neighbor shell are referred to by $-\nu$. Evaluating Eq. (23) for a hexagonal lattice with nearest-neighbor interactions we may use this notation to write

$$\Phi^0_{\alpha\beta}(-\nu) = \Phi^0_{\alpha\beta}(\nu) = -p_1(a)\delta_{\alpha\beta} - p_2(a)\hat{e}_{\nu\alpha}\hat{e}_{\nu\beta}, \tag{26}$$

with a being the lattice constant. $\Phi^0_{\alpha\beta}(00)$ then follows from Eq. (4). Using these expressions in Eq. (6) and introducing the abbrevation

$$c_\nu(\vec{q}) := 2[1 - \cos(\hat{\vec{e}}_\nu \cdot \vec{q}a)], \tag{27}$$

we can now write the dynamical matrix of a hexagonal lattice as follows:

$$D^0_{\alpha\beta}(\vec{q}) = -\sum_{\nu=1}^{3} \Phi^0_{\alpha\beta}(\nu) c_\nu(\vec{q}) = p_1(a)\delta_{\alpha\beta}\left[\sum_\nu c_\nu(\vec{q})\right] + p_2(a) \times \left[\sum_\nu \hat{e}_{\nu\alpha}\hat{e}_{\nu\beta} c_\nu(\vec{q})\right]. \quad (28)$$

B. Periodic substrate potential

We next determine $D^L_{\alpha\beta}(\vec{q})$ in Eq. (7). The hexagonal crystal is exposed to a periodic substrate potential U of the form $U(\vec{r}) = U_0[1-\cos(\vec{k}\cdot\vec{r})]$. Potentials of this shape can be realized experimentally by interfering two laser beams where both the wave vector $\vec{k}$ and the amplitude U_0 can be varied continuously. We here do not intend to discuss the problem in its full generality, but focus instead on the more practical case of commensurate structures where $\vec{k}$ is identical to a lattice vector $\vec{G}$ of the reciprocal lattice. This choice implies that the distance between two successive local minima of the substrate potential matches the distance between those neighboring lattice lines whose normal vector is parallel to $\vec{G}$. Thus, if only one lattice site is located in a local minimum of the substrate potential, then all sites of the crystal are located in such minima. It is obvious that the same minimum of the one-dimensional cosine function is occupied by all those sites which together form one common lattice line (from the set of lattice lines indexed by the vector $\vec{G}$). Expanding

$$U(\vec{r}) = U_0[1-\cos(\vec{G}\cdot\vec{r})] \quad (29)$$

about a lattice site $\vec{R}$ and remembering that $\vec{G}\cdot\vec{R} = 2\pi n$ with n being an integer, we obtain for a small displacement $\vec{u} = \vec{r} - \vec{R}$ the parabolic external potential,

$$U(\vec{u}) = \frac{U_0 G^2}{2}(\hat{\vec{G}}\cdot\vec{u})^2, \quad (30)$$

where $\vec{G} = G\hat{\vec{G}}$ with G being the absolute value of $\vec{G}$. Each particle of the crystal is thus exposed to a restoring external force along $\pm\hat{\vec{G}}$, which results from an external harmonic potential with a spring constant $U_0 G^2$.

In the following, we will consider a single substrate potential or a combination of two substrate potentials of the form of Eq. (30). These potentials are parametrized by $(U_0^1, \vec{G}_{\mu_1})$ and $(U_0^2, \vec{G}_{\mu_2})$ where $\mu_1, \mu_2 \in \{0,1,2,3,4\}$ refer to the vectors $\vec{G}_0 = \vec{0}$ and

$$\vec{G}_1 = G_1\vec{e}_x, \quad \vec{G}_2 = G_2\left(\frac{\sqrt{3}}{2}\vec{e}_x + \frac{1}{2}\vec{e}_y\right),$$

$$\vec{G}_3 = G_3\left(\frac{1}{2}\vec{e}_x + \frac{\sqrt{3}}{2}\vec{e}_y\right), \quad \vec{G}_4 = G_4\vec{e}_y, \quad (31)$$

where

$$G_1 = G_3 = \frac{4\pi}{\sqrt{3}a}, \quad G_2 = G_4 = \frac{4\pi}{a}. \quad (32)$$

The vector $\vec{G}_0$ is needed to describe the case where only one substrate potential is present. Equipped with this set of parameters, the potential energy V^L arising from the interaction between the substrate potential and the colloids may be written as

$$V^L = \frac{1}{2}\sum_l \{U_0^1[\vec{G}_{\mu_1}\cdot\vec{u}(l)]^2 + U_0^2[\vec{G}_{\mu_2}\cdot\vec{u}(l)]^2\}. \quad (33)$$

From Eq. (2), it then follows that $\Phi^L_{\alpha\beta}(ll')$ is diagonal in l and that $\Phi^L_{\alpha\beta}$ in Eq. (3) reads

$$\Phi^L_{\alpha\beta} = [U_0^1\vec{G}_{\mu_1}\vec{G}_{\mu_1} + U_0^2\vec{G}_{\mu_2}\vec{G}_{\mu_2}]_{\alpha\beta}. \quad (34)$$

From Eq. (6) we see that $D^L_{\alpha\beta}(\vec{q}) = \Phi^L_{\alpha\beta}$ and we finally arrive at the dynamical matrix of the full problem,

$$D_{\alpha\beta}(\vec{q}) = D^0_{\alpha\beta}(\vec{q}) + \Phi^L_{\alpha\beta}, \quad (35)$$

with $D^0_{\alpha\beta}(\vec{q})$ from Eq. (28) and $\Phi^L_{\alpha\beta}$ from Eq. (34).

C. Band structure and phonon spectrum

Diagonalizing Eq. (35) we obtain the set of eigenvalues $\lambda(\vec{q}j)$ which constitute the phonon band structure of our system. We consider the following six combinations of vectors $\vec{G}_{\mu_1}$ and $\vec{G}_{\mu_2}$ in Eq. (34):

	a	b	c	d	e	f
μ_1	1	0	1	1	1	2
μ_2	0	2	2	3	4	4

(36)

where the first line distinguishes the different cases and where the indices of the second and third lines refer to the vectors defined in Eqs. (31) and (32). In cases (a) and (b) the substrate potential has a modulation in just one direction while all other cases refer to situations with superposed modulations in two directions. It is evident from general symmetry considerations that case (a) comprises all possible cases with a modulation in just one direction and a $\vec{G}_{\mu_1}$ vector corresponding to a first-order Bragg peak. The same applies to case (b) with a $\vec{G}_{\mu_1}$ vector corresponding to a second-order Bragg peak. Cases (c)–(f), furthermore, list all possible combinations of the two modulations of cases (a) and (b). Therefore, the six cases considered here comprise all possible cases if one concentrates on modulations in two directions and first- and second-order Bragg peaks only.

All six cases are depicted in Fig. 2 showing the first Brillouin zone (BZ) of the reciprocal lattice. Also shown is the first BZ of a free crystal with the three high-symmetry points Γ, M, and K. As usual, band structures are visualized by plotting the bands along the axis of the BZ that join these symmetry points (thick solid line in Fig. 2). Note that this line circumvents that part of the BZ which is the smallest repeat unit of the band structure; it is the "irreducible section" of the BZ and comprises for the free crystal just 1/12th

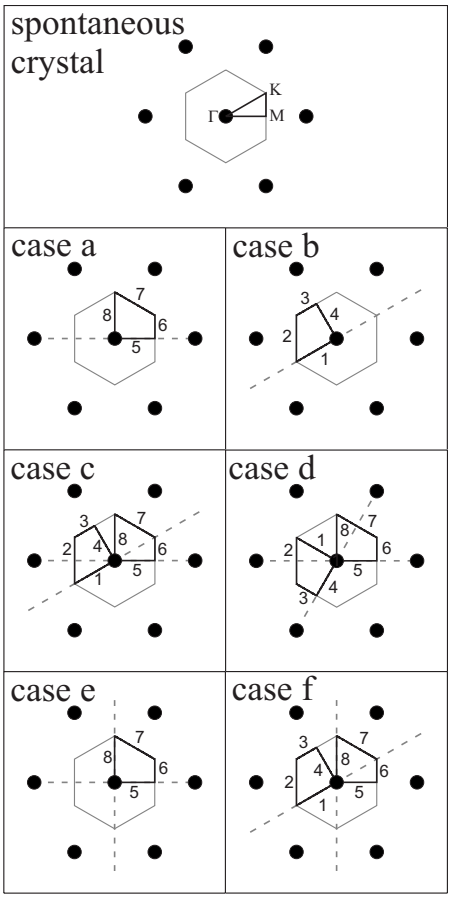

FIG. 2. The first Brillouin zone of the reciprocal lattice of a 2D hexagonal crystal (gray solid line), for a free crystal and for crystals subject to commensurate periodic potentials with modulations in different directions (dashed line). The path enclosing the irreducible section of the first Brillouin zone is plotted as a thick solid line. The numbers label the sections of this path along which the band structure is determined.

of the entire BZ. The substrate potential, though conserving the hexagonal symmetry of the lattice, leads to a reduction of the symmetry regarding the system of springs, with the effect that the irreducible section of the BZ increases. In case (a) [case (b)] the substrate potential has a sinusoidal modulation along the $\pm\hat{\hat{G}}_1$ [$\pm\hat{\hat{G}}_2$] direction (dashed lines in Fig. 2). The irreducible part of the BZ now comprises one-fourth of the total area of the BZ. Allowing for modulations along two directions as in cases (c)–(f), the irreducible section becomes as large as one-half of the BZ, with case (e) as the only exception where this section is again only one fourth of the BZ.

$D_{\alpha\beta}(\vec{q})$ depend on four parameters $p_1(a)$ and $p_2(a)$ from Eq. (24) and U_0^1/a^2 and U_0^2/a^2 in Eq. (34). It can be shown that $p_1(a)$ is small compared to $p_2(a)$ and that it has only a minor effect on the band structure [26]. In order to reduce the dimensionality of the parameter space, we set $p_1(a)$ to zero. Furthermore, we set $p_2(a)=k_0$ and take k_0 as a reference spring constant; i.e., we quantify $D_{\alpha\beta}(\vec{q})$ and the resulting band structure in terms of k_0. We are thus left with just two independent parameters

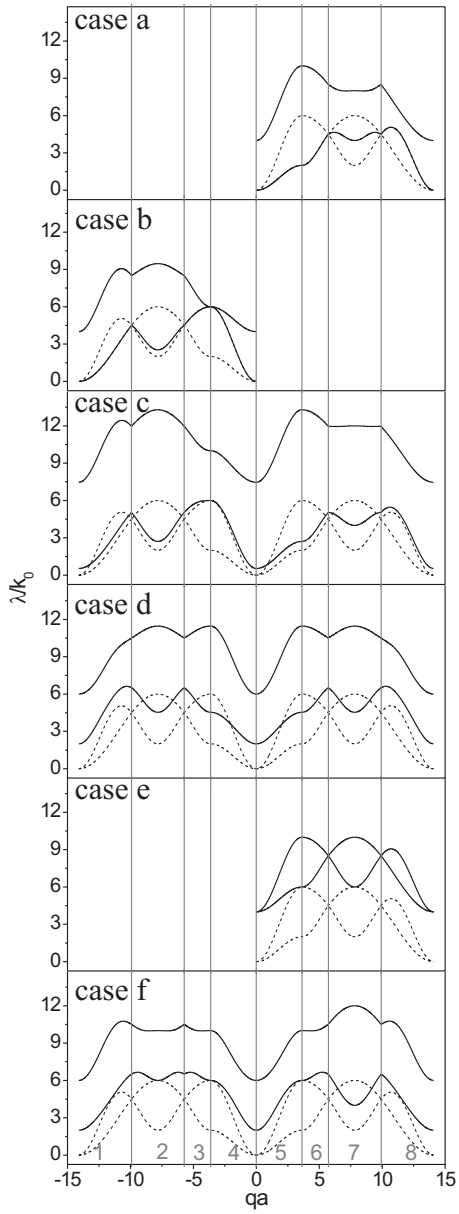

FIG. 3. Phonon band structures $\lambda(\vec{q}j)$ of a 2D hexagonal crystal (dashed line) and of a crystal subject to commensurate external potentials (solid line) for the six cases specified in Fig. 2. The gray numbers correspond to the numbers in Fig. 2, identifying the sections of the path along which $\lambda(\vec{q}j)$ is determined. $(k_1/k_0, k_2/k_0)$ is (4,0), (0,4), (4,4), (4,4), (4,4), (4,4) in (a)–(f).

$$k_1 = U_0^1(G_{\mu_1})^2, \quad k_2 = U_0^2(G_{\mu_2})^2, \tag{37}$$

with G_{μ_1} and G_{μ_2} from Eq. (32), depending on what case in (36) is considered. This permits us to study our problem quite generally for various combinations of k_1/k_0 and k_2/k_0.

Figure 3 shows the band structure for all six cases of Fig. 2, setting $k_1=4k_0$ and $k_2=0$ in case (a), $k_1=0$ and $k_2=4k_0$ in case (b), and $k_1=k_2=4k_0$ in cases (c)–(f). To highlight the effect caused by the substrate potential, we added to all graphs the band structure of the free crystal. On paths 5, 6, and 8 in case (a) [paths 1, 3, and 4 in case (b)] we observe that the shape of the band structure is not changed by the

substrate potential but that only one band is shifted while the position of the other has remained unaltered. Bands having polarization vectors (14) that point in a direction perpendicular to the direction of the modulation are not affected by the substrate potential. Consider, for example, a single modulation along the $\vec{e}_x$ direction—a situation that we have in case (a). The lower bands on paths 5 and 8 of the free crystal in Fig. 3(a) have polarization vectors that are perpendicular to $\vec{q}$ (transversal modes), thus pointing into the $\vec{e}_y$ direction on path 5 and in the $\vec{e}_x$ direction on path 8. It is clear then that a modulation in $\vec{e}_x$ direction shifts the transversal band upwards on path 8, but does not have an effect on the bands on path 5. Only on path 7 in case (a) [path 2 in (b)] does the substrate potential affect the shape of the bands; it flattens out the bands such that in case (a) almost no dispersion is left. Case (c) is a superposition of the substrate potentials in (a) and (b), and accordingly, the resulting band structure can to a good approximation be understood as a superposition of the structures in (a) and (b). Case (d) [case (f)] is a superposition of twice case (a) [case (b)], with the two superposed modulations being in two different directions (see Fig. 2). It is interesting to observe that although a complicated band structure arises in these cases, one can still identify sections where the bands are only shifted while its shape remains unchanged. Case (d) is symmetric about $qa=0$; this symmetry would not appear if $k_1 \neq k_2$. Rather special is case (e) ($k_1=k_2=4k_0$) where the superposed modulations of cases (a) and (b) are perpendicular to each other. Here, the whole band structure is just shifted by $4k_0$ while its shape is completely conserved. In other words, (e) represents a case where the substrate potential is tuned such that the resulting system of additional "springs" is again perfectly compatible with the hexagonal symmetry.

We next study the dependence of the band structure on k_1 and k_2 and take case (e) as an example. It is convenient to condense the band structures into a one-dimensional function, the phonon spectrum, defined as

$$G(\lambda) = \frac{1}{2N} \sum_{\vec{q}j} \delta(\lambda - \lambda(\vec{q}j)). \tag{38}$$

As this distribution is normalized to 1,

$$\int_0^\infty G(\lambda) d\lambda = 1, \tag{39}$$

we may interpret it as the fraction of eigenvalues of the dynamical matrix to be found in the interval $[\lambda, \lambda + d\lambda]$.

Figure 4 shows the band structures (left column) and phonon spectra (right column) for case (e) in Fig. 2. Figure 4(a) starts with the free crystal, in (b) and (c) k_1 is increased from 0 to $4k_0$ in steps of $2k_0$, and in (d) to (f) k_2 is then added, increasing to $6k_0$, again in steps of $2k_0$. In order to demonstrate the symmetry breaking of the band structures by the substrate, these graphs are complemented in Fig. 5 by two-dimensional contour plots of the band structures.

Figure 4(a) shows that each branch leads to one infinity in $G(\lambda)$ which can be fitted to the expression $\ln|\lambda - \lambda_c|$. These logarithmic singularities correspond to those parts in the band structure where $\lambda(\vec{q}j)$ has a saddle point. We have

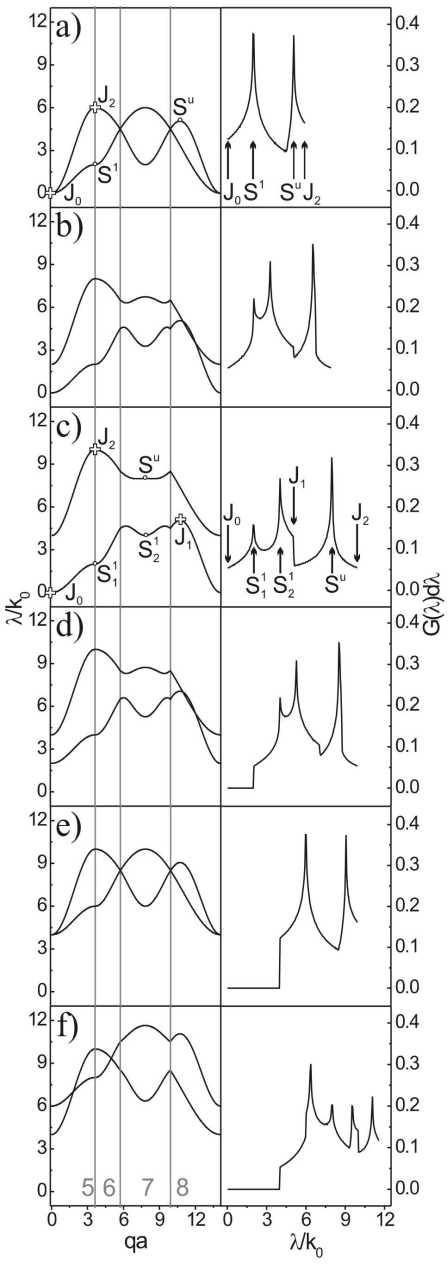

FIG. 4. Band structures for case (e) in Fig. 2 and corresponding phonon spectra, for various substrate potential strengths. $(k_1/k_0, k_2/k_0)$ is [from (a) to (f)] (0,0), (2,0), (4,0), (4,2), (4,4), (4,6). The gray numbers correspond to the numbers in Fig. 2, case (e), identifying the sections of the path along which $\lambda(\vec{q}j)$ is determined.

marked these saddle points by solid circles and the labels S^1 and S^u in the band structure plots of Fig. 4 and the contour plots of Fig. 5. Minima and maxima in $\lambda(\vec{q}j)$ lead to jump singularities. Crosses and labels J_0, J_1, and J_2 mark these points in the band structures. The phonon spectrum of Fig. 4(a) shows furthermore a sharp kink between the two peaks which result from the points where the upper and lower bands touch each other.

In going from Fig. 4(a) to Fig. 4(c) we start to decouple the bands and $G(\lambda)$ decomposes into two (still overlapping) parts $G_L(\lambda)$ and $G_H(\lambda)$, one for each band. The part $G_H(\lambda)$

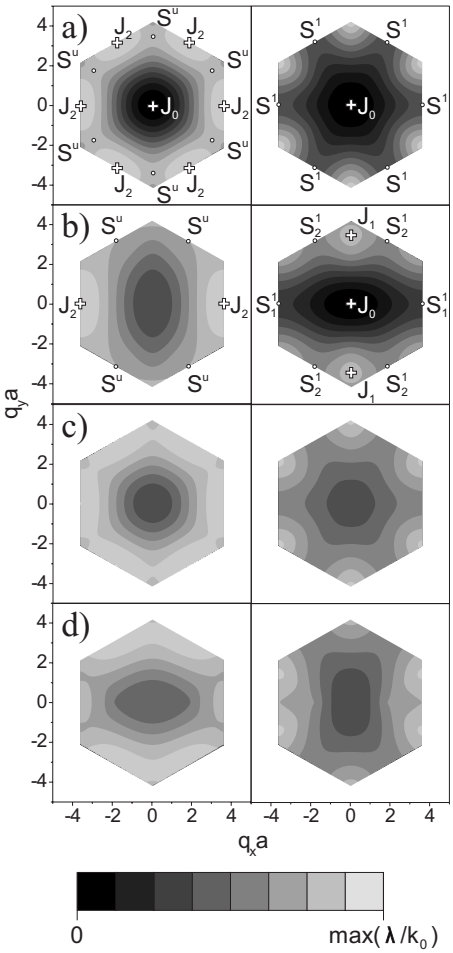

FIG. 5. 2D contour plots of the band structure in the first Brillouin zone for case (e) in Fig. 2 and for the following combinations of $(k_1/k_0, k_2/k_0)$: (0,0), (4,0), (4,4), (4,6) from (a) to (d). (a) is the free crystal; (b) represents also case (a) of Fig. 2. The left (right) column of graphs displays the higher (lower) bands.

for the higher band shows one logarithmic divergence [corresponding to the saddle point S^u marked in Fig. 5(b) and the band structure of Fig. 4(c)] and two jump singularities which result from the two maxima J_1 and J_2, which we have also marked in the band structures. The part $G_L(\lambda)$ for the lower band shows a splitting of initially one logarithmic singularity into two such singularities. This reflects the fact that the six degenerate saddle points of type S^1 in Fig. 5(a) split into two saddle points of type S_1^1 and four saddle points of type S_2^1 [see Fig. 5(b)]. In Fig. 4(d) then k_2 takes a nonzero value, resulting in a shift of $G_L(\lambda)$ to higher λ, such that a further increase of k_2 to $k_1=k_2=4k_0$ leads in (e) to a phonon spectrum which is again the spectrum of (a), just shifted to the right by $\lambda=4k_0$. Note that also the spectrum in (d) is the same as that in (b), just that it is shifted by $2k_0$. Hence, in (a)–(c) one substrate potential produces a perturbation whose effect in (d) and (e) the second substrate potential is able to cancel again (except for the shift of the entire band structure). A more complicated phonon spectrum with several singularities is produced in (f) when k_2 is further increased so that the two band systems heavily interpenetrate each other. The band structures of (f) are also shown as contour plots in Fig. 5(d). If all four pictures of Fig. 5 are seen as a sequence—$(k_1/k_0, k_2/k_0)$ is (0,0), (4,0), (4,4), (4,6)—we observe in (b) a reshaping of the band structure in the x direction and then on increasing k_2 first a restoration of the structure of (a) in (c), followed in (d) by a reshaping in the y direction when k_2 is stronger than k_1.

V. WAYS TO PROBE THE BAND STRUCTURE

Ways to access experimentally the phonon band structure of colloidal crystals are discussed in this section. The first idea is to determine the phonon spectrum from a measurement of the mean-square displacement (MSD) of the colloids in the crystal. We demonstrate in the following section that phonon spectrum and MSD are related to each other by a Laplace transformation.

A. Relation between phonon spectrum and mean-square displacement

We return to the Langevin equation in the $(\vec{q}j)$ representation, Eq. (22). It has the formal solution

$$Q(t) = Q_0 e^{-(\lambda/\gamma)t} + e^{-(\lambda/\gamma)t}\frac{1}{\gamma}\int_0^t e^{(\lambda/\gamma)t'}F(t')dt', \qquad (40)$$

where for clarity we have suppressed $(\vec{q}j)$ in the arguments of Q, Q_0, F, and λ. Using this expression and exploiting Eq. (18), we can calculate the phonon autocorrelation function

$$\langle Q(t+\tau)Q^*(t)\rangle = \left\{\langle|Q_0|^2\rangle - \frac{\epsilon}{2\lambda\gamma}\right\}e^{-(\lambda/\gamma)(2t+\tau)} + \frac{\epsilon}{2\lambda\gamma}e^{-(\lambda/\gamma)\tau}, \qquad (41)$$

where $\langle\cdots\rangle$ denotes the ensemble average. Realizing that equipartition must apply for $\tau=0$ and $t\to\infty$ we can evaluate the constant ϵ and obtain

$$\epsilon = 2\gamma kT, \qquad (42)$$

and hence Eq. (41) becomes

$$\langle Q(t+\tau)Q^*(t)\rangle = \frac{kT}{\lambda}e^{-(\lambda/\gamma)\tau} + e^{-(\lambda/\gamma)2t} \times\left\{\langle|Q_0|^2\rangle e^{-(\lambda/\gamma)\tau} - \frac{kT}{\lambda}e^{-(\lambda/\gamma)\tau}\right\}. \qquad (43)$$

We observe for $\tau=0$ that $\langle|Q|^2\rangle$ starts from $\langle|Q_0|^2\rangle$ and approaches its equipartition value kT/λ within a time period roughly given by $\gamma/(2\lambda)$. For $\tau>0$, kT/λ is not approached, but the smaller value $e^{-\lambda\tau/\gamma}kT/\lambda$. For times larger than $\gamma/(2\lambda)$, we may thus approximate Eq. (43) by the simple expression

$$\langle Q(t+\tau)Q^*(t)\rangle \approx \frac{kT}{\lambda}e^{-(\lambda/\gamma)\tau}. \qquad (44)$$

Having this in mind, we now turn to the quantity

$$c(\tau) = \langle \vec{u}(t+\tau) \cdot \vec{u}(t) \rangle_l$$
$$= \frac{1}{N} \sum_{l,\alpha} \langle u_\alpha(l,t+\tau) u_\alpha(l,t) \rangle$$
$$= \frac{1}{N} \sum_{\vec{q},j} \langle Q(\vec{q}j,t+\tau) Q^*(\vec{q}j,t) \rangle, \quad (45)$$

where we used Eqs. (9), (11), and (12). The index l at $\langle \cdots \rangle_l$ serves as a reminder that in addition to the ensemble average, an average over all lattice sites is to be performed. Writing this expression with $G(\lambda)$ defined in Eq. (38) and inserting Eq. (44), we arrive at

$$c(\tau) = \int d\lambda G(\lambda) \frac{2kT}{\lambda} e^{-(\lambda/\gamma)\tau}. \quad (46)$$

The time-dependent MSD $\delta_{\mathrm{MSD}}(\tau)$ is defined as

$$\delta_{\mathrm{MSD}}(\tau) = \langle |\vec{u}(t+\tau) - \vec{u}(t)|^2 \rangle_l = 2[c(0) - c(\tau)], \quad (47)$$

with $c(\tau)$ from Eq. (45). With Eq. (46) we obtain

$$\delta_{\mathrm{MSD}}(\infty) = 2c(0) = 4kT \int d\lambda \frac{G(\lambda)}{\lambda}, \quad (48)$$

relating the phonon spectrum to the absolute MSD. The physical meaning of $c(\tau)$ now becomes obvious from

$$c(\tau) = \frac{1}{2}[\delta_{\mathrm{MSD}}(\infty) - \delta_{\mathrm{MSD}}(\tau)] = 2kT \int d\zeta \frac{G(\gamma\zeta)}{\zeta} e^{-\zeta\tau}. \quad (49)$$

Writing $c(\tau)$ in this form we recognize that it can be understood as the Laplace transform of $G(\lambda)/\lambda$. In that sense, the Laplace transform of the phonon spectrum is directly related to the time-dependent MSD. Thus one experimental way to get access to the phonon band structure is by first measuring the time-dependent MSD in order to determine the function $c(\tau)$ and by then applying the inverse Laplace transform of $c(\tau)$ to obtain $G(\lambda)/\lambda$.

Expressing Eq. (49) in reduced quantities $\tau' = \tau k_0/\gamma$ and $\lambda' = \lambda/k_0$ using the reference spring constant k_0, we obtain

$$\frac{k_0 c(\tau)}{kT} = 2 \int d\lambda' \frac{G(\lambda')}{\lambda'} e^{-\lambda'\tau'}. \quad (50)$$

Figure 6 shows $\delta_{\mathrm{MSD}}(\tau)$ and $\delta_{\mathrm{MSD}}(\infty)$ in these units. The time-dependent MSD in (a) is obtained from integrating the phonon spectra plotted in Fig. 4. A logarithmic behavior is observed for the first three cases where $k_2 = 0$ and a saturation behavior is found for the last three cases where both substrate potentials have a finite strength. Figure 4 reveals that $G(0) = 0$ in the last three cases, while $\lim_{\lambda \to 0} G(\lambda) \neq 0$ in cases (a)–(c) which according to Eq. (48) must lead to a logarithmic divergence of $\delta_{\mathrm{MSD}}(\infty)$. In other words, the logarithmic behavior of the MSD we observe in Fig. 6(a) can be associated with the jump singularity of $G(\lambda)$ at $\lambda = 0$. Only if this jump singularity is shifted away from $\lambda = 0$ does the MSD reach a finite level as in cases (d)–(f).

This finite level of the MSD $\delta_{\mathrm{MSD}}(\infty)$ is plotted in Fig. 6(b) as a function of k_1/k_0 at fixed $k_2 = 4k_0$ for the six cases

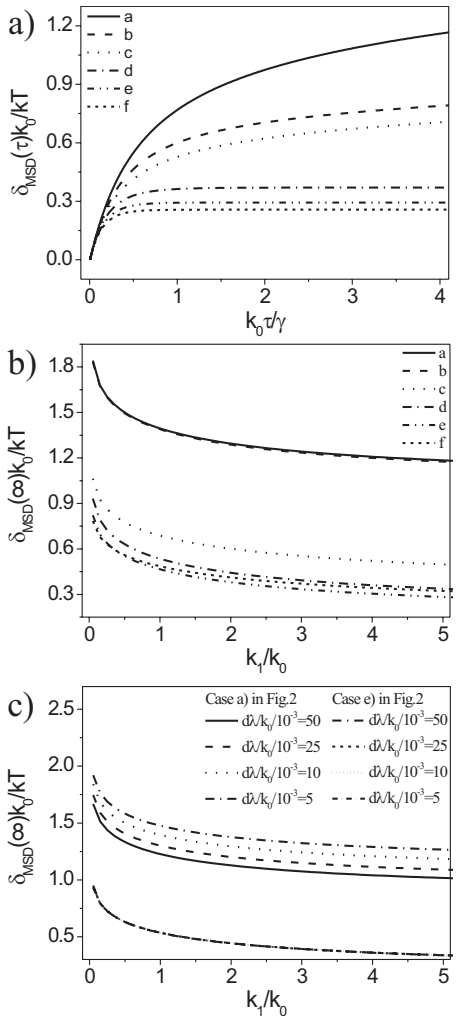

FIG. 6. (a) Time dependence of the mean-square displacement $\delta_{\mathrm{MSD}}(\tau)$ for the six cases considered in Fig. 4. (b) Mean-square displacement $\delta_{\mathrm{MSD}}(\infty)$ as a function of the strength k_1 of the substrate potential for the six cases specified in Fig. 2. If required, k_2 is set to $4k_0$. (c) shows for cases (a) and (e) in Fig. 2 the dependence of $\delta_{\mathrm{MSD}}(\infty)$ on the bin size $d\lambda$ of the phonon spectrum $G(\lambda)$ for four different bin sizes (see plot legend for details).

specified in Fig. 2. $\delta_{\mathrm{MSD}}(\infty)$ is generally the lower the stronger the substrate potential is; it also decreases in going from (a) and (b) to cases (c)–(f) when the movement of the particles is further confined by the second substrate potential. However, we hasten to stress that the curves of cases (a) and (b) in Fig. 6(b) are not converged, but depend on the bin size $d\lambda$ chosen in the integration of Eq. (48). This is illustrated in Fig. 6(c) where $\delta_{\mathrm{MSD}}(\infty)$ is computed using different bin sizes. We observe that the results of case (e) of Fig. 2 do not depend on the bin size while those for case (a) show such a dependence. The figure reveals that $\delta_{\mathrm{MSD}}(\infty)$ is in fact infinity in cases (a) and (b), in agreement with what we have already observed in Fig. 6(a).

The logarithmic divergence of $\delta_{\mathrm{MSD}}(\infty)$ displays the well-known effect [27–29] that long-wavelength fluctuations [or, equivalently, the jump singularity of $G(\lambda)$ at $\lambda = 0$] in 2D crystals lead to an instability. As a consequence of this effect, a 2D crystal has no true long-range order, but only a quasi-

long-range order characterized by an algebraic decay of the translational correlation function [4]. Figure 6, in essence, demonstrates that modulations in two directions are required to cure this instability because only modulations in two directions are capable of shifting the jump singularity of $G(\lambda)$ away from $\lambda=0$. Modulations in just one direction will inevitably lead to such a singularity at $\lambda=0$ because one band of the free crystal will always remain unaffected by the presence of the substrate potential which is enough to let $G(\lambda)$ jump at $\lambda=0$. We should also remark that k_1 and k_2 do not need to have a value above a certain threshold in order to overcome the instability, but that it suffices to demand that $k_1>0$ and $k_2>0$ in order to prevent $\delta_{\mathrm{MSD}}(\infty)$ from diverging.

Returning finally to Fig. 4, we recall the observation that in (a)–(c) one substrate potential produces a disturbance whose effect in (d) and (e) the second substrate potential is able to cancel, restoring the original system of springs of the free crystal. One is then tempted to think that the shift of the phonon spectrum is immaterial. However, we now understand that this picture is incomplete as it ignores the important stabilizing effect which arises as the result of the shift of the phonon spectrum.

B. Direct determination of the band structure

The most direct way to get experimentally access to the band structure results from exploiting the equipartition theorem which demands that every term in the sum of Eq. (15) have on average an energy $kT/2$. Hence,

$$\lambda(\vec{q}j)\langle|Q(\vec{q}j)|^2\rangle = kT, \tag{51}$$

which Eq. (14) allows us to rewrite as

$$\lambda(\vec{q}j) = \frac{kT}{\langle|\vec{e}^*(\vec{q}j)\cdot\vec{u}(\vec{q})|^2\rangle}. \tag{52}$$

The video-microscopy technique records the displacements $\vec{u}(l)$ of all colloidal particles of a crystalline configuration from which we can easily evaluate the right-hand side of Eq. (52). In that way, band structures of colloidal crystals have been determined in Refs. [1,30,31].

An alternative way to measure $\lambda(\vec{q}j)$ has not yet been experimentally realized. It is based on Eq. (44) which we can rewrite to define a normalized phonon autocorrelation function

$$y(\vec{q}j,\tau) = \frac{\langle Q(\vec{q}j,t+\tau)Q^*(\vec{q}j,t)\rangle}{\langle|Q(\vec{q}j)|^2\rangle} = e^{-\lambda(\vec{q}j)\pi/\gamma}. \tag{53}$$

These functions can again be directly evaluated from video-microscopy data and allow us to determine the phonon decay times

$$T(\vec{q}j) = \frac{\gamma}{\lambda(\vec{q}j)}, \tag{54}$$

from which we can again gain access to $\lambda(\vec{q}j)$. Note that this equation corresponds to what is known as a "dispersion relation" in atomic systems, relating frequencies to wave vectors. In our case, the overdamped limit, we have to relate relaxation times to wave vectors. Ohshima and Nishio [25] therefore refer to this equation as the "overdamped dispersion relation."

VI. ELASTICITY AND BEHAVIOR AT LONG WAVELENGTHS

A. Elasticity

This section addresses the question whether or not it is possible to tune the elastic behavior of colloidal crystals by means of the substrate potential. Starting from the theory of lattice dynamics we get to the elastic constants by applying the method of homogeneous deformation; see [32]. We subject all particles in the lattice to a linear homogeneous transformation

$$R'_\alpha(l) = R_\alpha(l) + \sum_\beta u_{\alpha\beta}R_\beta(l), \tag{55}$$

with the constants $u_{\alpha\beta}$ being the deformation parameters. This equation implies that

$$u_\alpha(l) = \sum_\beta u_{\alpha\beta}R_\beta(l). \tag{56}$$

The elastic constants can now be derived by calculating the change in potential energy caused by this deformation. The total potential energy is the sum of V^0 and V^L, with V^L given by Eq. (33) which we rewrite as

$$V^L = \frac{1}{2}\sum_{i=1}^{2} U_0^i \sum_{l,\alpha,\beta} G_{\mu_i,\alpha}G_{\mu_i,\beta}u_\alpha(l)u_\beta(l). \tag{57}$$

Let us denote the new potential energy by $V'=V^{0\prime}+V^{L\prime}$. Inserting Eq. (56) into Eq. (57), we obtain, for $V^{L\prime}$,

$$V^{L\prime} = \frac{1}{2}\sum_{\alpha,\beta,\gamma,\lambda} C^L_{\alpha\beta\gamma\lambda}u_{\alpha\gamma}u_{\beta\lambda}, \tag{58}$$

where

$$C^L_{\alpha\beta\gamma\lambda} = \sum_{i=1}^{2} U_0^i \sum_l G_{\mu_i,\alpha}G_{\mu_i,\beta}R_\gamma(l)R_\lambda(l) \tag{59}$$

can be interpreted as the change in the elastic constants caused by the substrate potential. Depending on the choice of the two vectors $\vec{G}_{\mu_1}$ and $\vec{G}_{\mu_2}$, the constants $C^L_{\alpha\beta\gamma\lambda}$ are either zero or infinity. For those constants that are zero, we may conclude that the substrate potential has no effect at all on the corresponding deformation such that the elastic constants are those of the free crystal, while for all other constants, the presence of the substrate potential inhibits the corresponding deformation from occurring. We observe that the circumstance that $C^L_{\alpha\beta\gamma\lambda}$ can become infinity results from the quadratic dependence of V^L on $u_\alpha(l)$—a dependence that itself arise from an expansion which is valid only for small displacements. Using the full expression (29) in our analysis we would avoid this divergence. Still the resulting constants would depend on U_0^1 and U_0^2—i.e., the energy barrier between neighboring lattice lines. Only in that sense are the

constants tunable by the substrate potentials. However, for practical reasons, these barriers should be chosen high enough (larger than a few kT) to prevent thermally excited colloids from crossing them. This in practice means that the elastic constants are at least one order of magnitude larger than those of the free crystal.

B. Expanding the dynamical matrix

To provide an approximate analytic expression for the band structure near the center of the BZ, we next expand the dynamical matrix in Eq. (35) about $\vec{q}=0$. We start by considering $D^0_{\alpha\beta}(\vec{q})$ from Eq. (28). Recalling the defining equation (6) and expanding this expression up to second order, we obtain

$$D^0_{\alpha\beta}(\vec{q}) = -\frac{1}{2}\sum_{l,\gamma,\lambda} \Phi^0_{\alpha\beta}(0l)R_\gamma(l)R_\lambda(l)q_\gamma q_\lambda, \tag{60}$$

where the zeroth-order term vanishes because of Eq. (4) while the first-order term is identical to zero because of the symmetry of the lattice and Eq. (26). Inserting Eq. (23) into Eq. (60) results in

$$D^0_{\alpha\beta}(\vec{q}) = v_a \sum_{\gamma,\lambda} [C^0_{\alpha\beta\gamma\lambda} - p\,\delta_{\alpha\beta}\delta_{\gamma\lambda}]q_\gamma q_\lambda, \tag{61}$$

where $v_a=\sqrt{3}a^2/2$ is the area of the unit cell and p is the pressure while

$$C^0_{\alpha\beta\gamma\lambda} = \frac{1}{2v_a}\sum_l p_2(R(l))\frac{R_\alpha(l)R_\beta(l)R_\gamma(l)R_\lambda(l)}{R^2(l)} \tag{62}$$

are the elastic constants of the free crystal. A colloidal crystal with purely repulsive interaction requires a finite pressure in order not to explode. Therefore, the stress tensor has nonzero diagonal elements given by p,

$$T_{\gamma\lambda} = -p\,\delta_{\gamma\lambda} = \frac{1}{2v_a}\sum_l p_1(R(l))R_\gamma(l)R_\lambda(l), \tag{63}$$

an equation that we have already used in Eq. (61). Since $C^0_{1111}-p=2\mu+\lambda$ and $C^0_{1122}-p=\mu$ with μ and λ being the two Lame coefficients, we can finally write down $D^0_{\alpha\beta}(\vec{q})$,

$$\mathbf{D}^0(\vec{q}) \approx v_a\begin{pmatrix} (2\lambda+\mu)q_x^2+\mu q_y^2 & 2(\mu+p)q_xq_y \\ 2(\mu+p)q_xq_y & \mu q_x^2+(2\lambda+\mu)q_y^2 \end{pmatrix}, \tag{64}$$

recalling that $C^0_{1111}=C^0_{2222}$, $C^0_{1122}=C^0_{1212}=C^0_{2211}$ and that $C^0_{1211}=C^0_{2111}=C^0_{1222}=C^0_{2122}=0$. In other words, in the $\vec{q}=q_x\vec{e}_x$ direction and in the $\vec{q}=q_y\vec{e}_y$ direction, the two bands decouple and have a parabolic form $v_a\mu q^2$ and $v_a(2\lambda+\mu)q^2$.

The second term in Eq. (35) is $\Phi^L_{\alpha\beta}$ which is not dependent on $\vec{q}$, so that the whole matrix has to be added to Eq. (64) to obtain an approximation of $D_{\alpha\beta}(\vec{q})$. Approximate expressions for the bands then follow from the eigenvalues of this matrix. For example, choosing the $\vec{q}=q_x\vec{e}_x$ direction, $D_{\alpha\beta}(\vec{q})$ is given by

$$\mathbf{D}(\vec{q}) \approx \begin{pmatrix} D_{11}(q) & \Phi^L_{12} \\ \Phi^L_{12} & D_{22}(q) \end{pmatrix} \tag{65}$$

in the neighborhood of $q=0$ with $D_{11}(q)=\Phi^L_{11}+v_a(2\lambda+\mu)q^2$ and $D_{22}(q)=\Phi^L_{22}+v_a\mu q^2$. The two bands are then given by

$$\lambda(\vec{q},\pm) \approx \frac{1}{2}\{D_{11}(q)+D_{22}(q) \pm \sqrt{[D_{11}(q)+D_{22}(q)]^2-4[D_{11}(q)D_{22}(q)-(\Phi^L_{12})^2]}\}. \tag{66}$$

VII. SUMMARY AND CONCLUDING REMARKS

In this paper we have explored 2D colloidal crystals that are exposed to commensurate substrate potentials and studied how the colloidal lattice dynamics can be changed, tuned and manipulated by means of these potentials. We have calculated the phonon band structure for various different combinations of external modulations. To take account of the substrate potentials the dynamical matrix of the free crystal must be supplemented by an additional $\vec{q}$-independent matrix $\Phi^L_{\alpha\beta}$ whose elements can be selectively controlled by changing the strength of the potentials but also the direction of the modulations.

We summarize our observations as follows. Substrate potentials (i) break the symmetry of the band structure within the first Brillouin zone, from its initial sixfold hexagonal symmetry to the symmetry of the substrate potential, (ii) decouple bands by shifting one band while leaving the other unaffected, and (iii) can be used to change the shape of individual bands, in cases so effectively that no band dispersion remains. For two substrate potentials with modulations in the perpendicular direction, one can tune the substrate potentials such that the whole band structure is just shifted while its shape is completely conserved. In these cases, one substrate potential produces a perturbation whose effect on the shape of the bands is canceled by the second substrate potential; the resulting system of additional "springs" is then again compatible with the hexagonal symmetry. The only effect that remains is a shift of the whole band structure and the corresponding phonon spectrum. This includes a shift of an important jump singularity of this spectrum near $\lambda=0$—a shift which we have seen requires modulations in at least two directions to occur. The shift of this jump singularity expresses the fact that the crystal becomes locked into the substrate potential's periodicity, thus acquiring perfect long-range order. This then allows the mean-square displacement of the colloids to remain finite. The study of the phonon spectra has revealed that new jump singularities can be created and that a splitting of initially one logarithmic singularity into two such singularities can occur.

We have discussed various methods to experimentally investigate the predicted effects. Two-dimensional colloidal suspensions subjected to substrates created by interfering laser beams and observed with a microscope allow direct de-

termination of the band-structure via the equipartition theorem or, alternatively, the measurement of the phonon decay times via an analysis of the phonon autocorrelation functions. Another experimental way to get access to the phonon band structure is by measuring the time-dependent MSD and exploiting the fact this quantity is directly related to the Laplace transform of the phonon spectrum, a relation that we here have established starting from the Langevin equation for colloidal crystals. We have finally shown that the elastic constants of the crystal cannot be tuned; they are either not affected by the substrate potential or affected that strongly that they effectively suppress the corresponding homogeneous deformation.

ACKNOWLEDGMENTS

The authors would like to thank Clemens Bechinger for initiating this work, for his ongoing input, and for his hospitality in summer 2006. This work was supported by the Austrian Science Foundation (FWF, Project No. 18762).

[1] P. Keim, G. Maret, U. Herz, and H. H. von Grünberg, Phys. Rev. Lett. **92**, 215504 (2004); H. H. von Grünberg, P. Keim, K. Zahn, and G. Maret, *ibid.* **93**, 255703 (2004).
[2] K. Zahn, J. M. Mendez-Alcaraz, and G. Maret, Phys. Rev. Lett. **79**, 175 (1997); K. Zahn, R. Lenke, and G. Maret, *ibid.* **82**, 2721 (1999); K. Zahn and G. Maret, *ibid.* **85**, 3656 (2000).
[3] D. R. Nelson, *Phase Transitions and Critical Phenomena* (Academic, London, 1983).
[4] L. W. Bruch, M. W. Cole and E. Zaremba, *Physical Adsorption, Forces and Phenomena* (Clarendon Press, Oxford, 1997).
[5] D. G. Grier, Nature (London) **424**, 810 (2003).
[6] A. Chowdhury, B. J. Ackerson, and N. A. Clark, Phys. Rev. Lett. **55**, 833 (1985).
[7] J. Chakrabarti, H. R. Krishnamurthy, A. K. Sood, and S. Sengupta, Phys. Rev. Lett. **75**, 2232 (1995).
[8] Q. H. Wei, C. Bechinger, D. Rudhardt, and P. Leiderer, Phys. Rev. Lett. **81**, 2606 (1998).
[9] C. Bechinger and E. Frey, J. Phys.: Condens. Matter **13**, R321 (2001).
[10] S. Bleil, M. Brunner, J. Dobnikar, R. Castaneda-Priego, H. H. von Grünberg, and C. Bechinger, Europhys. Lett. **73**, 450 (2006).
[11] J. Baumgartl, M. Brunner, and C. Bechinger, Phys. Rev. Lett. **93**, 168301 (2004).
[12] C. Bechinger, M. Brunner, and P. Leiderer, Phys. Rev. Lett. **86**, 930 (2001).
[13] K. Mangold, P. Leiderer, and C. Bechinger, Phys. Rev. Lett. **90**, 158302 (2003).
[14] M. Brunner and C. Bechinger, Phys. Rev. Lett. **88**, 248302 (2002).
[15] R. Piazza and V. Degiorgio, Phys. Rev. Lett. **67**, 3868 (1991).
[16] A. J. Hurd, N. A. Clark, R. C. Mockler, and W. J. O'Sullivan, Phys. Rev. A **26**, 2869 (1982).
[17] J. Derksen and W. van de Water, Phys. Rev. A **45**, 5660 (1992).
[18] M. Hoppenbrouwers and W. van de Water, Phys. Rev. Lett. **80**, 3871 (1998).
[19] B. V. R. Tata, P. S. Mohanty, M. C. Valsakumar, and J. Yamanaka, Phys. Rev. Lett. **93**, 268303 (2004).
[20] J. T. Padding and A. A. Louis, Phys. Rev. E **74**, 031402 (2006).
[21] B. V. R. Tata, in *Flow Dynamics: The Second International Conference on Flow Dynamics*, edited by M. Tokuyama and S. Maruyama, AIP Conf. Proc. No. 832 (AIP, New York, 2006), p. 91.
[22] P. Schram, A. G. Sitenko, and V. I. Zasenko, Physica B **228**, 197 (1996).
[23] B. U. Felderhof and R. B. Jones, Z. Phys. B: Condens. Matter **64**, 393 (1986).
[24] M. Born and K. Huang, *Dynamical Theory of Crystal Lattices* (Clarendon Press, Oxford, 1956).
[25] Y. N. Ohshima and I. Nishio, J. Chem. Phys. **114**, 8649 (2001).
[26] The experimental system most promising to experimentally verify our ideas uses charged-stabilized colloidal suspensions where the colloidal particles interact via a screened Coulomb potential. Inserting typical values for the relevant parameters leads to the result that $p_1/p_2 < 0.1$.
[27] R. E. Peierls, Helv. Phys. Acta **7**, Supp. II, 81 (1934).
[28] Y. Imry and L. Gunther, Phys. Rev. B **3**, 3939 (1971).
[29] Y. Imry, Crit. Rev. Solid State Mater. Sci. **8**, 157 (1978).
[30] J. Zhanghellini, P. Keim, and H. H. von Grünberg, J. Phys.: Condens. Matter **17**, S3579 (2005).
[31] D. Reinke, H. Stark, H. H. von Grünberg, A. B. Schofield, G. Maret, and U. Gasser, Phys. Rev. Lett. 98, 038301 (2007).
[32] Born and Huang [24], Chap. 3.